Anisotropy in structural and physical properties in tetrathiafulvalene derivatives-based zone-cast layers as seen by Raman spectroscopy, UV-visible spectroscopy, and field effect measurements

Sylwia Kotarba, Jaroslaw Jung, Aneta Kowalska, Tomasz Marszalek, Marcin Kozanecki et al.

Related Articles

Triisopropylsilylethynyl-functionalized anthradithiophene derivatives for solution processable organic field effect transistors
Appl. Phys. Lett. 101, 043301 (2012)

The high-pressure electronic structure of the [Ni(ptdt)2] organic molecular conductor
J. Chem. Phys. 137, 024701 (2012)

Functional K-doping of eumelanin thin films: Density functional theory and soft x-ray spectroscopy experiments in the frame of the macrocyclic protomolecule model
J. Chem. Phys. 136, 204703 (2012)

Exciton transport in organic semiconductors: Förster resonance energy transfer compared with a simple random walk
J. Appl. Phys. 111, 044510 (2012)

Solution doping of organic semiconductors using air-stable n-dopants
APL: Org. Electron. Photonics 5, 54 (2012)

Additional information on J. Appl. Phys.

Anisotropy in structural and physical properties in tetrathiafulvalene derivatives-based zone-cast layers as seen by Raman spectroscopy, UV-visible spectroscopy, and field effect measurements

Sylwia Kotarba,[1,a)] Jaroslaw Jung,[1] Aneta Kowalska,[1] Tomasz Marszalek,[1] Marcin Kozanecki,[1] Pawel Miskiewicz,[1] Marta Mas-Torrent,[2] Concepció Rovira,[2] Jaume Veciana,[2] Josep Puigmarti-Luis,[2] and Jacek Ulanski[1]

[1]*Department of Molecular Physics, Technical University of Lodz, 90-924 Lodz, Poland*
[2]*Institut de Ciència de Materials de Barcelona (CSIC), Campus Universitari de Bellaterra, 08193 Cerdanyola del Vallès, Spain*

We have studied anisotropy of thin layers of amphiphilic tetrathiafulvalene derivatives (TTF-4SCn, with n=12, 18, and 22) obtained by zone-casting technique. All the films show optical anisotropy, as seen by polarized optical microscopy and polarized UV-visible spectroscopy. By using polarized Raman spectroscopy an angular dependence of intensity of different vibrational modes in respect to the zone-casting direction was determined. It was found that intensities of the modes related to central and ring C=C vibrations in the TTF core depend very strongly on the angle between the zone-cast direction and polarization plane of incident laser light. Comparison of the deduced orientation of the molecules in one of the films (TTF-4SC18) with its crystal structure shows that the polarized Raman spectroscopy can be useful for controlling orientation of molecules in thin films (e.g., for online monitoring). Organic field effect transistors (OFETs), with channels oriented in parallel and perpendicularly to the zone-casting direction, were built using the oriented TTF-4SCn films. In all cases a strong anisotropy of the charge carrier mobility (μ) was found; the best results were obtained for OFETs with TTF-4SC18, for which $\mu_{\parallel}=0.25$ cm^2/V s, ON/OFF$>10^5$, and $\mu_{\parallel}/\mu_{\perp}\approx170$. © *2010 American Institute of Physics*. [doi:10.1063/1.3311554]

I. INTRODUCTION

Several small π-conjugated molecules show strong tendency for quasi-one-dimensional π-stacking resulting in high charge carrier mobility along the stacks. In order to employ such materials in organic electronics it is necessary to elaborate effective methods of producing large area oriented thin layers of organic semiconductors. This aspect is one of the challenging tasks for the fabrication of organic field effect transistors (OFETs), since well ordered thin films will result in intermolecular $\pi-\pi$ overlapping and, consequently, in high charge carrier mobility along a preferred direction, that is along the device channel. Equally important is the elaboration of a quick and possibly simple technique for the control of both the molecules' orientation and the molecular stacks in such anisotropic layers.

In recent years it was demonstrated that the so-called zone-casting method can be successfully applied to produce unidirectional aligned thin layers of different types of organic semiconductors, such as p and n type organic crystals or discotic liquid crystals without the use of any preoriented substrates.[1–6] We have reported the preparation of high performance OFETs based on zone-cast large area aligned films of DT-TTF an amphiphilic tetrathiafulvalene (TTF) derivative, namely, tetrakis-(octadecylthio)-tetrathiafulvalene (TTF-4SC18).[7–15]

Unique properties of semiconducting symmetrical TTF derivatives are tightly connected with their ability of piling up molecules one after another.[16–18] The single crystals structure analysis exhibits strong influence of the alkyl chain substituent on to the molecular packing. Depending on the substituent alkyl chain length the molecular conformation changes from boatlike to chairlike structure and the single crystals have various forms (plates or needles), different colors, and other physical properties.[19] By increasing the alkyl chain length, the ability to form perfect single crystals strongly decreases, so for the derivatives with the chain length higher than n=11 defected needlelike crystals are usually observed and it was not possible to determine their crystal structures.[20,21]

TTF-4SC18 molecules assemble into one-dimensional stacks in which the long alkyl chains promote intermolecular $\pi-\pi$ overlapping acting as so-called molecular fasteners.[16,22] This is because of the van der Waals interactions between the alkyl chains fasten the TTF cores of neighboring molecules tightly along the stacks.[23] The structure of the zone-cast films was characterized by synchrotronic x-ray diffraction, indicating an extremely high crystalline quality.

In independent studies carried out by means of the polarized Raman microspectroscopy on single crystals of different TTF derivatives' salts, it was found that two main vibration modes, ν_2 and ν_3, corresponding to the central C=C vibrations and the ring C=C vibrations, respectively, demonstrate high sensitivity on the orientation of laser polarization plane in respect to the orientation of the molecules.[24,25] This has inspired us to apply the polarized
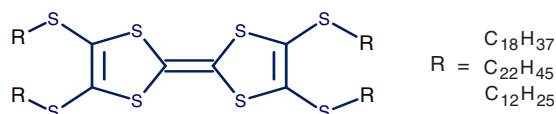
a)Electronic mail: s.kotarba@p.lodz.pl.

FIG. 1. (Color online) Molecular structure of tetrakis(alkylthio)tetrathiafulvalenes (TTF-4SCn, where n=12, 18, or 22).

FIG. 2. (Color online) Scheme of the top contact OFET devices; channel length $L=80,100$ μm; channel width $W_\perp=1.5$ mm or $W_\parallel=2$ mm for the channel perpendicular and parallel to the cast direction, respectively; U_{DS}—drain-source voltage, U_{GS}—gate voltage, I_{DS}—drain-source current.

Raman spectroscopy for determination of orientation of the TTF derivatives molecules in the zone-cast layers.

In this paper we characterize the zone-cast layers of a series of TTF derivatives with alkyl chains of different lengths showing how the polarized Raman spectroscopy can be used to determine orientation of the molecules in the layers. Complementary investigations by means of atomic force microscope (AFM) and polarized UV-visible spectroscopy are also shown. Anisotropy of charge carrier transport properties is demonstrated by determining the OFET mobility in two directions that is along the zone-casting direction and perpendicularly to it.

II. EXPERIMENTAL

A. Material

The structure of the TTF-4SCn (n=12, 18, 22) molecules is shown on Fig. 1. These molecules were synthesized as described by Wu *et al.*[26] Thermal properties of different TTF derivatives change with the alkyl chain length. The derivatives investigated in this work have melting points: T_m =68 °C (TTF-4SC12), T_m=87.7 °C (TTF-4SC18), and T_m =89 °C (TTF-4SC22).[27]

B. Preparation of large area oriented films and OFET structure

In the zone-casting method the solution of the organic molecules is continuously cast from stationary flat nozzle on to a moving substrate; gradient of the parameters controlling the crystallization (concentration and temperature) in the meniscus is the driving force for unidirectional crystallization of the dissolved material. Preparation of well ordered, continuous layers of organic semiconductors requires optimization of several factors: type of solvent, concentration and temperature of solution, speed of solution supply, properties and temperature of the substrate, and velocity of the substrate shift. In the present studies the solutions were prepared using toluene (for TTF-4SC18) and chlorobenzene (for TTF-4SC12 and TTF-4SC22). The solutions concentration was 2 mg/ml. Highly doped *n*-type silicon wafer (gate) with 100 nm thermally grown silicon dioxide (Si/SiO$_2$) were used as substrates.[28] For polarized UV-visible absorption spectra measurements the layers were zone-cast on glass substrates. The large area (about 3×10 cm^2) highly ordered, continuous films with thickness about ~250 nm were obtained after careful optimization of the casting parameters for each TTF derivative.

The OFETs with top contact bottom gate configuration (see Fig. 2) were produced by evaporation of 150 nm thick gold electrodes (source and drain) on the zone-cast layers with channels parallel and perpendicular to the casting direction. Channel length was $L=80$ μm or $L=100$ μm; channel
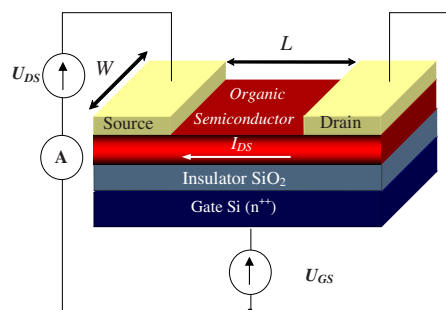
width W=2 mm and W=1.5 mm were chosen for channels aligned in parallel or perpendicularly for perpendicular to the casting direction, respectively.

C. Characterization techniques

Uniformity of the optical anisotropy of the zone-cast layers was studied by polarized optical microscope. Morphology of the surface was investigated by AFM (AFM SOLVER PRO, NT-MDT, Russia) in resonant mode. Polarized UV-visible absorption spectra were obtained using Varian Cary 5000 ultraviolet-visible-near infrared (UV-visible-NIR spectrometer).

Polarized Raman spectra in the range 1300–1600 cm^{-1} were obtained using a Jobin–Yvon T64000 Raman microscope working in backscattering mode. For the calibration of the spectrometer the diamond line (1332 cm^{-1}) was used. The angular dependence of the spectra was determined by rotation of the sample with 10° step in respect to the fixed polarized excitation laser light. The measurements were performed twice using 632 and 647 nm excitation lines with spectral resolution of 2 cm^{-1} and 1200 s accumulation time.

Transfer and output electrical characteristics were measured for series of OFETs with channel perpendicular and parallel to the cast direction. Figure 2 shows the scheme of the measurement circuit. By using two Keithley 2400 source-measuring units the drain-source current (I_{DS})-voltage (U_{DS}) characteristics were measured [output characteristic I_{DS} =f(U_{DS}) with U_{GS}=const.]. Drain-source voltage U_{DS} was changed in the range 0 to −40 V with step ΔU_{DS}=−5 V (for TTF4SC12 and TTF4SC22) and with step ΔU_{DS}=−2 V for TTF4SC18; gate voltage U_{GS} was changed in the range +5 to −40 V.

Transfer characteristics [I_{DS}=f(U_{GS}) with U_{DS}=const.] were measured with gate voltage U_{GS} changing in the range +5 to −40 V with step ΔU_{GS}=−5 V with drain-source voltage fixed U_{DS}=−40 V. Mobility of charge carriers μ_{OFET} was calculated from saturation regime using the formula,

$$\mu_{\text{OFET}} = 2I_{\text{DSAT}}L[WC_i(U_{GS} - U_T)^2]^{-1}, \quad (1)$$

where I_{DSAT}-drain-source saturation current, L-channel length, W-channel width, C_i-capacitance per unit area, U_{GS}-gate voltage, and U_T-threshold voltage.
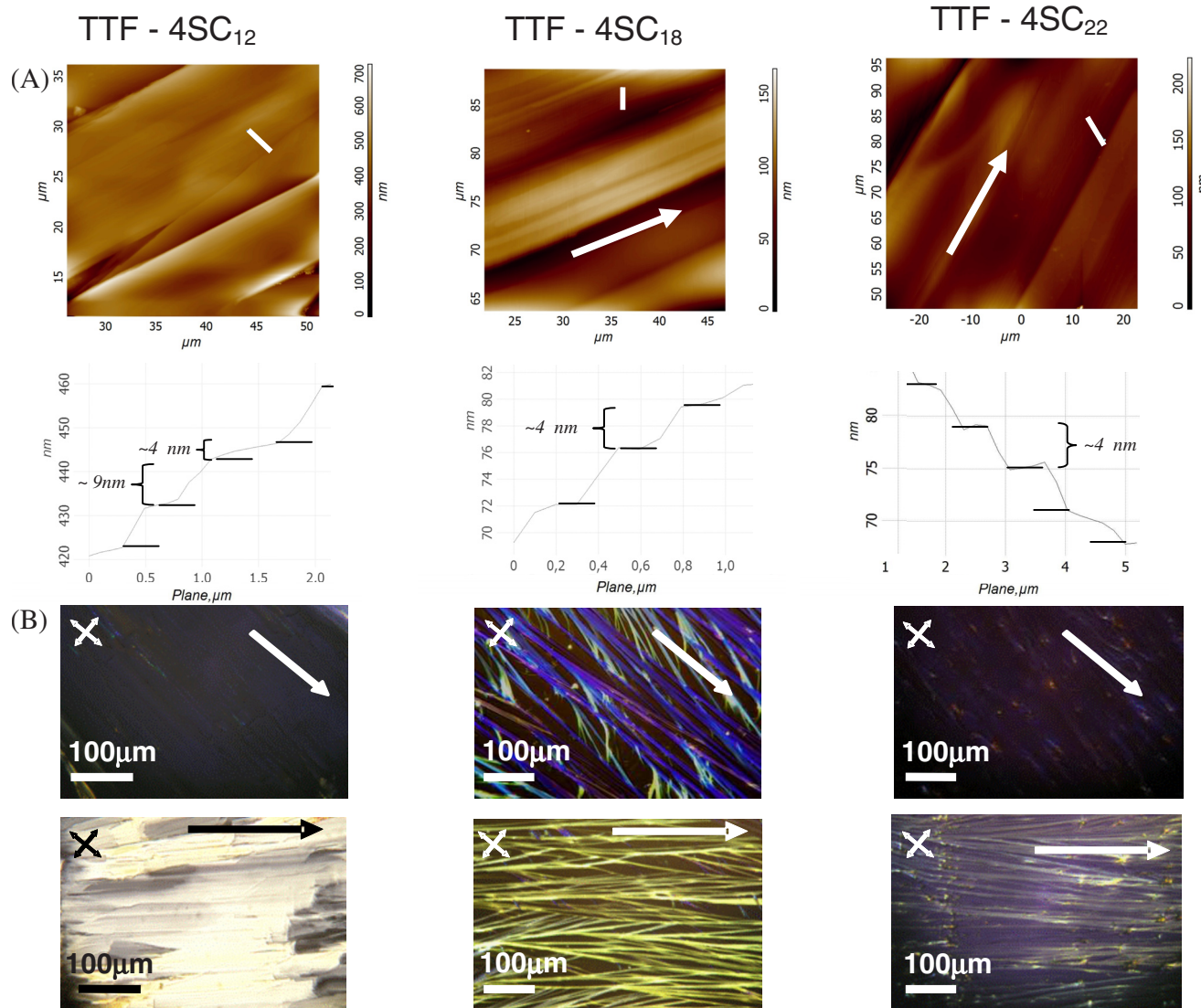
FIG. 3. (Color online) Top rows (a): morphology of the zone-cast layers of three TTF derivatives visualized by AFM images (resonant mode; top images) and related surface profiles illustrating the height of the terraces. The profiles are referred to white lines on AFM images. Bottom rows (b): polarizing microscope images with crossed polarizers for two different orientations of the layers in respect to light polarization plane; white arrow—zone-casting direction, crossed arrows—orientation of the polarization planes of the polarizers.

III. RESULTS AND DISCUSSION

Figure 3 shows AFM and polarized optical microscope images of the zone-cast layers of three investigated TTF derivatives. One can clearly see that morphology shows anisotropy on both micrometer and millimeter scales; in fact such anisotropic morphology is uniform for the entire 3×10 cm^2 layer (except for the regions very close to the edges).

AFM images show that surface of the layers is smooth along the casting direction, while in the perpendicular direction a terracelike structure is seen, with step heights in nanometer scale. Our previous studies focused on the TTF-4SC18 layers on Si/Si$_3$N$_4$/SiO$_2$ have shown that the steps are ca. 4–5 nm in height, corresponding this value to the lattice parameter b perpendicular to the surface ($b=41.8$ Å; crystal structure was determined from x-ray diffraction experiments performed at the beamline ID01 of the European Synchrotron Radiation Facility).[11] As this parameter is smaller than the TTF-4SC18 molecule length (ca. 53 Å) it

was concluded that the molecules are tilted in respect to the surface by ca. $55 \pm 10°$. As one can see from the surface profiles shown in Fig. 3, the steps height in all three cases are around 4 nm, indicating that the terraces are constituted by monomolecular layers of TTF derivative molecules tilted with respect the substrate surface.

Optical anisotropy, visible both on the polarized optical images obtained in reflection mode (Fig. 3) and in the UV-visible polarized absorption spectra (Fig. 4), demonstrates homogeneous orientation of the molecules in the entire layers. For all these oriented layers the polarized UV-visible spectra show a strong dependence band, at 415 nm, on the orientation of the layer in respect to the light polarization plane. In the case of TTF-4SC18, the orientation of molecules inside the layer, determined by the crystallographic studies, indicates that the molecules tend to form stacks parallel to the film surface with the long molecular axis oblique in respect to the substrate surface, as mentioned above.[11] Band at the 425 nm, visible in UV-visible spectra for all

TTF-4SC12

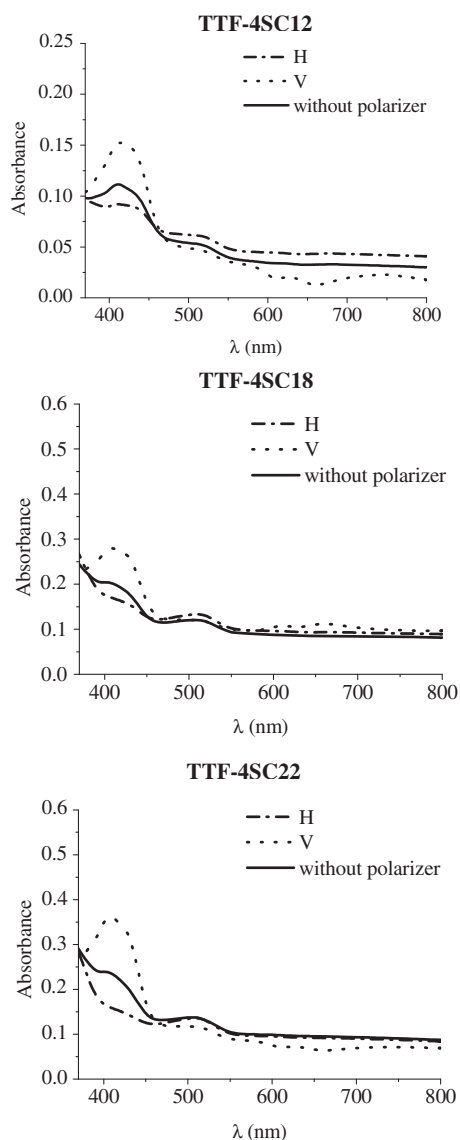**TTF-4SC18**

TTF-4SC22

FIG. 4. Polarized UV-visible spectra of the oriented thin films based on TTF derivatives obtained by zone-casting technique on glass substrates; V—polarization plane perpendicular to the zone-casting direction, H—polarization plane parallel to the zone-casting direction. For comparison the spectra obtained without polarizer are also shown.

layers of TTF derivatives, is the strongest for the perpendicular direction, i.e., for the direction approximately parallel to short axis of the TTF core. As the polarized UV-visible spectra for other TTF derivatives are similar, one can conclude that the orientation of the molecules in all these zone-cast layers is similar.

The above described results illustrate anisotropic structures of the zone-cast layers and unidirectional orientation of the TTF derivatives molecules. In order to get more information on the orientation of the molecules we have analyzed the vibrational spectra using the polarized Raman spectroscopy. We have focused our attention on two main vibration modes of the TTF core: the ν_2, mode related to the central C=C vibrations, and the perpendicularly oriented ν_3 mode, related to the ring C=C vibrations, as shown in Fig. 5(a).

Taking into account that in the Raman spectra of bis(ethylenedithitertrathiafulvalene) (BEDT-TTF, in which the cen-

tral part has a similar structure to the TTF core in the investigated TTF derivatives) the ν_3 band appears at 1494 cm^{-1}, and the ν_2 band at 1552 cm^{-1} one can expect that the bands related to the analogous vibrations in the TTF derivatives will appear also in the similar range.[14] To confirm this, the density functional theory (DFT) calculations were performed for model TTF derivatives with different lengths of the SC_xH_y chains. The molecular geometry of the neutral molecules was first optimized by the DFT method using the scheme B1-LYP employing the Gaussian basis set [6-31G(d)] for each atom. Chairlike structure of the TTF derivatives is shown in the inset in Table I. Based on these optimized structures the vibrational analyses were realized by using GAUSSIAN 98 program software package. DFT simulations were carried out for the BEDT-TTF and for the family of the TTF derivatives starting from central core [B1LYP/ 6-31G(d)] and ending on the TTF core with four short SC_4H_9 chains [ONIOM (B1LYP/6-31G(d):PM3)].[30,31]

Results of the DFT simulations are compared with the available experimental data for frequencies of the ν_2 and ν_3 bands in Table I. One can observe that according to the DFT simulations, the frequency of the ν_2 mode is practically not sensitive to the presence of the SC_xH_y chains. On the contrary the frequency of the ν_3 mode shifts toward lower values as the length of the SC_xH_y chains is increased. However, this trend saturates for chains equal or longer than SC_2H_5. Taking this into account, one can assume that the DFT simulations for the investigated TTF derivatives ought to give similar results; therefore, we can assign the observed Raman bands at ca. 1560 cm^{-1} to the ν_2 mode and at ca. 1490 cm^{-1} to the ν_3 mode, as given in the Table I.[29]

Figure 5(b) shows the polarized Raman spectra for the oriented layer of TTF-4SC18 in the range 1300–1600 cm^{-1}, where two bands assigned to the ν_2 and ν_3 modes dominate. One can see that intensities of these two bands show very strong and clear dependence on the orientation of the light polarization plane in respect to the zone-casting direction. Similar angular dependences of the Raman spectra in this frequency range were observed for the zone-cast layers of TTF-4SC12 and TTF-4SC22. The most peculiar feature of these spectra is the fact that maximum intensity of the ν_2 band coincides with minimum intensity of the ν_3 band and vice versa.

Angular dependences of intensity of the ν_2 and ν_3 bands in the polarized Raman spectra for all the investigated zone-cast TTF derivatives are showed in polar coordinates in Fig. 6. For comparison, we have performed analogous measurements for single crystals of the TTF derivatives. The results are shown in Fig. 6 too. From the angular dependences of the intensity of the ν_2 and ν_3 bands one can deduce that in the zone-cast layers the molecules have unidirectional orientation, as schematically shown on the left side of Fig. 6. This is in an agreement with the results of crystallographic studies for the zone-cast layer of TTF-4SC18, which show an extremely high crystalline quality and indicate that the TTF molecules are tilted with respect to the substrate surface and are well-aligned in the casting direction.[11]

The situation is different for single crystals, as the plots of the angular dependences of the ν_2 and ν_3 bands are
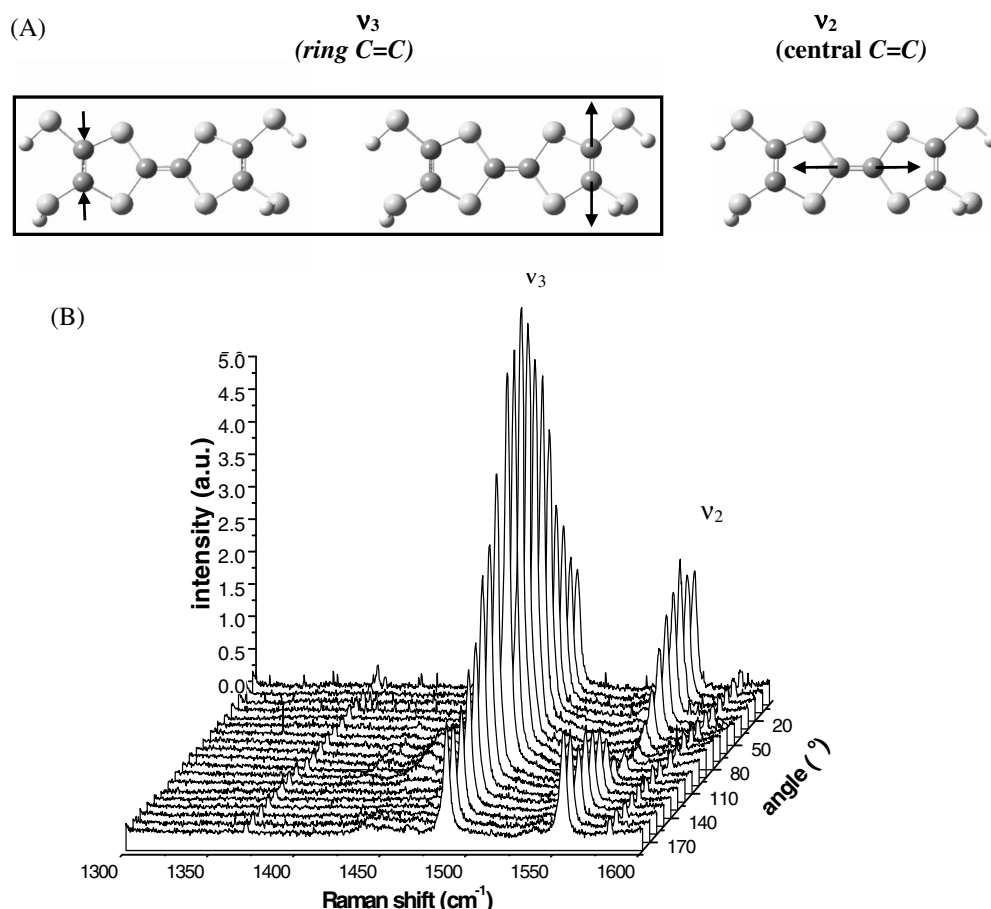
FIG. 5. (a) Vibrational ν_2 and ν_3 modes of the TTF-4SCn, cf. Table I. (b) Polarized Raman spectra for the zone-cast layer of TTF-4SC18 as a function of the angle between the zone-casting direction and the light polarization plane.

broader or even in some cases the plots have bimodal character showing that in the crystal there are two groups of the molecules oriented in two different directions. The reason for this can be either that these are not single but twin crystals or that the crystal structure of the zone-cast film is different from the bulk crystal structure. Unfortunately the structure of the bulk crystals of the TTF derivatives with long alkyl chains is so strongly defective, that it was not possible to determine their crystal structure [the structure of the TTF derivative with longest alkyl chain n=9 was only determined (see Fig. 6 in Ref. 19)]. However, we have shown earlier that the powder diffraction spectrum for the TTF-4SC18 shows the (0n0) Bragg peaks clearly shifted with respect to the peaks found in the reflectivity measurement for the zone-cast films. This indicates that the zone-cast film structure deviates from the bulk crystalline structure and shows a lower degree of disorder within the molecular layers.

Since the molecular stacks are laterally and vertically closely packed and well ordered, one can expect both high charge carrier mobility along the stacks and high anisotropy, i.e., much lower mobility along the directions perpendicular to the stacks. It is known that boundaries between neighbor crystals[32] strongly influence the mobility. Field effect measurements for devices with channels oriented in parallel and perpendicularly to the casting directions have confirmed this. In Fig. 7 the typical transfer characteristics for OFETs based

on zone-cast layers of the TTF derivatives and the related basic OFET parameters calculated using Eq. (1) have been reported.

The performance of the manufactured OFETs can be summarized as follows:
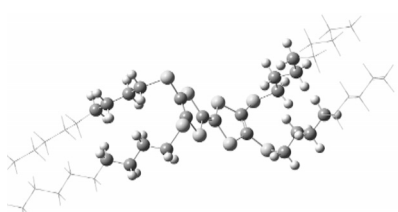
(a)   for all the TTF derivatives, the best device parameters are obtained for the OFETs with channel's length oriented along the zone-casting directions;

(b)   the highest charge carrier mobility, $\mu_\parallel$=0.25 cm^2/V s, the highest ON/OFF ratio, >10^5, and the highest anisotropy, $\mu_\parallel/\mu_\perp \sim$ 160, was obtained for OFETs based on TTF-4SC18;

(c)   in all cases the anisotropy of charge carrier mobility was much higher than any values reported even for OFETs based on single crystals.[33,34]

One should underline that the analyzed OFETs produced show good yield and reproducibility; for each ca. 3 ×10 cm layers more than ten OFETs were obtained and more than 90% of them were working showing performance close to those given in Fig. 7.

IV. CONCLUSIONS

Zone-casting technique is a relatively simple, solution-based method which allows to produce in a continuous way large area of highly ordered films based on crystalline or-

TABLE I. The theoretically calculated (DFT) and experimentally determined from Raman spectra vibrational frequencies assigned to the ν_2 and ν_3 modes for a series of TTF derivatives [cf. Fig. 5(a)].

Schematic chair-like structure of TTF-4SCn molecule.

	Vibrational modes	Frequencies calculated using DFT (cm^{-1})	Experimental data from Raman spectra (cm^{-1})
BEDT-TTF	ν_3	1518	1494 [ref. 29]
	ν_2	1566	1552 [ref. 29]
TTF-4S	ν_3	1516	-
	ν_2	1570	
TTF-4SC1	ν_3	1501	-
	ν_2	1567	
TTF-4SC2	ν_3	1498	-
	ν_2	1566	
TTF-4SC3	ν_3	1497	-
	ν_2	1566	
TTF-4SC4	ν_3	1498	-
	ν_2	1566	
TTF-4SC12	ν_3	-	1493
	ν_2		1559
TTF-4SC18	ν_3	-	1488
	ν_2		1556
TTF-4SC22	ν_3	-	1489
	ν_2		1556

[a]Reference 29.

ganic semiconductors. The zone-cast layers of the TTF derivatives show remarkable high degree of uniform alignment, as documented by polarized optical microscopy, AFM images, and polarized UV-visible spectra.
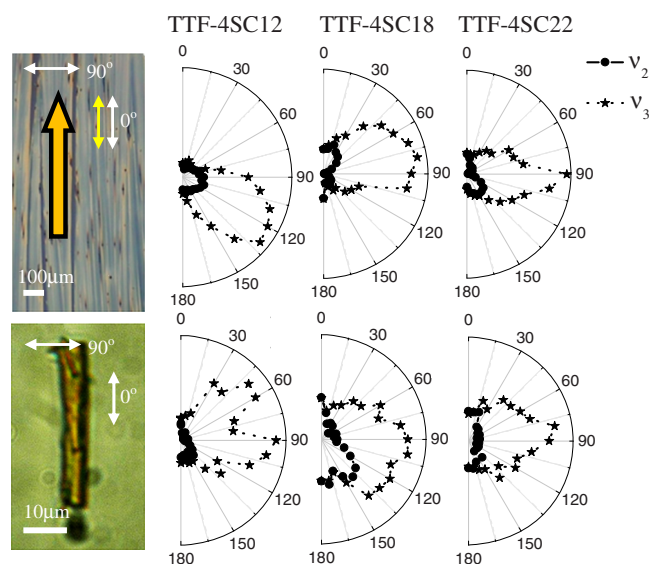

FIG. 6. (Color online) Angular dependences of the two main vibrational modes (the central C=C vibrations ν_2 and the ring C=C vibrations ν_3) for the analyzed TTF derivatives determined by polarized Raman spectroscopy in the range 1300–1600 cm^{-1}. Upper row—the zone-cast thin layers; 0° corresponds to the zone-casting direction shown by large arrow, as illustrated on the micrograph of the TTF-4SC22 layer. Lower row—the single crystals; 0° corresponds to long axes of the crystal, as illustrated on the micrograph of the TTF-4SC12 crystal.
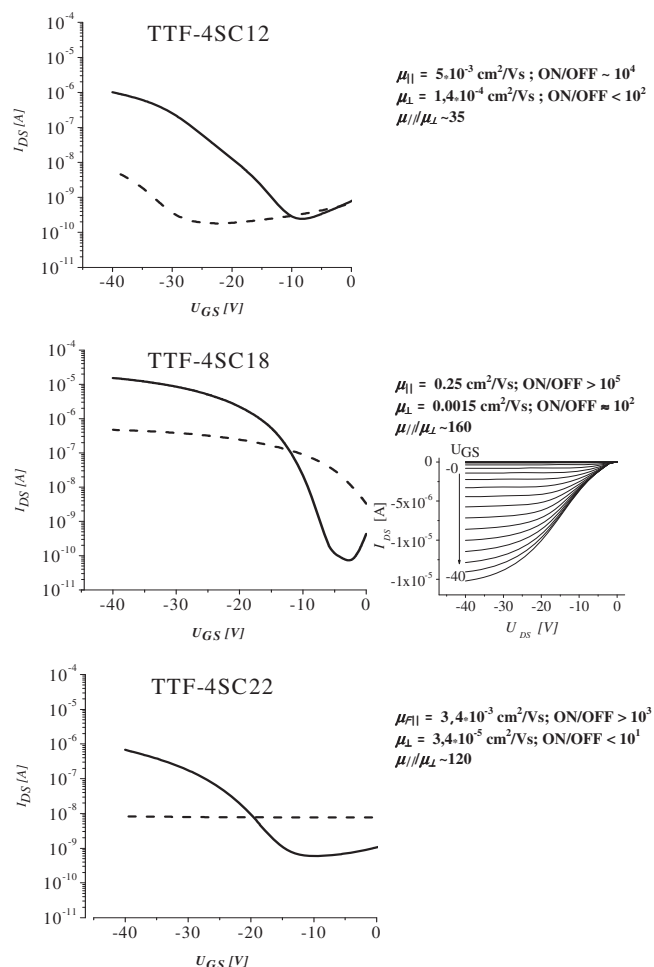

FIG. 7. Typical transfer characteristics and basic parameters of OFETs made of layers of TTF derivatives, acting as device channel, zone cast on SiO$_2$/Si substrates (cf. Fig. 2). Solid lines—channel parallel to the zone-casting direction, broken lines—channel perpendicular to the zone-casting direction. Channel length was in all cases $L_{\parallel}=L_{\perp}=80$ μm, except of TTF-4SC18 where $L_{\parallel}=100$ μm; channel widths were in all cases: $W_{\parallel}=2$ mm and $W_{\perp}=1.5$ mm. For TTF-4SC18 also the output characteristic is shown as an example.

Polarized Raman spectroscopy gives evidences of unidirectional orientation of the molecules, which in the zone-cast layers are uniformly and much better ordered on large area than in the corresponding single crystals. This demonstrates also that polarized Raman spectroscopy can be a useful technique for controlling the molecular order in organic crystalline materials, suitable also for monitoring online the quality of the produced thin layers of organic semiconductors.

The electrical characterization of OFETs based on the zone-cast layers of the TTF derivatives shows that due to the close packing and the effective overlapping of π-orbitals along the stacks, the charge carrier mobility in this direction can be as high as $\mu_{\parallel}=0.25$ cm^2/V s, and the ON/OFF ratio can be higher than 10^5. These measurements show also a very high anisotropy of the charge carrier mobility, higher than 10^2, that demonstrates high degree of unidirectional orientation of the stacks. For this reason, one can expect that even closely packed OFETs produced on the zone-cast layers should show no cross-talking effects.

[1] J. A. Lim, H. S. Lee, W. H. Lee, and K. Cho, Adv. Funct. Mater. **18**, 1 (2008).

[2] Q. Tang, Y. Tong, W. Hu, Q. Wan, and T. Bjornholm, Adv. Mater. (Weinheim, Ger.) **21**, 4234 (2009).

[3] N. Liu, Y. Zhou, L. Wang, J. Peng, J. Wang, J. Pei, and Y. Cao, Langmuir **25**, 665 (2009).

[4] D. H. Kim, D. Y. Lee, H. S. Lee, W. H. Lee, Y. H. Kim, J. I. Han, and K. Cho, Adv. Mater. (Weinheim, Ger.) **19**, 678 (2007).

[5] J. Y. Lee, S. Roth, and Y. W. Park, Appl. Phys. Lett. **88**, 252106 (2006).

[6] L. Jiang, W. Hu, Z. Wei, W. Xu, and H. Meng, Adv. Mater. (Weinheim, Ger.) **21**, 3649 (2009).

[7] M. Mas-Torrent, S. Masirek, P. Hadley, N. Crivillers, N. S. Oxtoby, P. Reuter, J. Veciana, C. Rovira, and A. Tracz, Org. Electron. **9**, 143 (2008).

[8] P. Miskiewicz, A. Rybak, J. Jung, I. Glowacki, W. Maniukiewicz, A. Tracz, J. Pfleger, J. Ulanski, and K. Müllen, Nonlinear Opt., Quantum Opt. **37**, 207 (2007).

[9] H. Sirringhaus, Adv. Mater. (Weinheim, Ger.) **21**, 3859 (2009).

[10] A. Tracz, J. Ulanski, T. Pakula, and M. Kryszewski, Polish Patent No. 231177 (1981).

[11] P. Miskiewicz, M. Mas-Torrent, J. Jung, S. Kotarba, I. Glowacki, E. Gomar-Nadal, D. B. Amabilino, J. Veciana, B. Krause, D. Carbone, C. Rovira, and J. Ulanski, Chem. Mater. **18**, 4724 (2006).

[12] L. Burda, A. Tracz, T. Pakula, J. Ulanski, and M. Kryszewski, J. Phys. D: Appl. Phys. **16**, 1737 (1983).

[13] P. Miskiewicz, A. Rybak, J. Jung, I. Glowacki, J. Ulanski, Y. Geerts, M. Watson, and K. Mullen, Synth. Met. **137**, 905 (2003).

[14] W. Pisula, A. Menon, M. Stepputat, I. Lieberwirth, U. Kolb, A. Tracz, H. Sirringhaus, T. Pakula, and K. Mullen, Adv. Mater. (Weinheim, Ger.) **17**, 684 (2005).

[15] A. Tracz, T. Makowski, S. Masirek, W. Pisula, and Y. H. Geerts, Nanotechnology **18**, 485303 (2007).

[16] H. Inokuchi, G. Saito, P. Wu, K. Seki, T. B. Tang, T. Mori, K. Imaeda, T. Enoki, Y. Higuchi, K. Inaka, and N. Yasuoka, Chem. Lett. **1986**, 1263.

[17] M. Mas-Torrent, P. Hadley, S. T. Bromley, X. Ribas, J. Tarres, M. Mas, E. Molins, J. Veciana, and C. Rovira, J. Am. Chem. Soc. **126**, 8546 (2004).

[18] M. Mas-Torrent and C. Rovira, J. Mater. Chem. **16**, 433 (2006).

[19] K. Imaeda, T. Enoki, Z. Shi, P. Wu, N. Okada, H. Yamochi, G. Saito, and H. Inokuchi, Bull. Chem. Soc. Jpn. **60**, 3163 (1987).

[20] C. Nakano, K. Imaeda, T. Mori, Y. Maruyama, H. Inokuchi, N. Iwasawa, and G. Saito, J. Mater. Chem. **1**, 37 (1991).

[21] C. Nakano, T. Mori, K. Imaeda, N. Iwasawa, and G. Saito, Bull. Chem. Soc. Jpn. **65**, 2086 (1992).

[22] G. Saito, Pure Appl. Chem. **59**, 999 (1987).

[23] G. Saito and Y. Yoshida, Bull. Chem. Soc. Jpn. **80**, 1 (2007).

[24] R. Wojciechowski, "Raman Spectroscopy of anions in conducting and superconducting single crystals and composites of Bis(ethylene-dithio)tetrathiafulvalene trihalides," Lodz (2000).

[25] A. Graja, *Spectroscopy of Materials for Molecular Electronics* (Scientific, Poznan, 1997).

[26] P. Wu, G. Saito, K. Imaeda, Z. Shi, T. Mori, T. Enoki, and H. Inokuchi, Chem. Lett. **1986**, 441.

[27] Z. Shi, T. Enoki, K. Imaeda, K. Seki, P. Wu, H. Inokuchi, and G. Saito, J. Phys. Chem. **92**, 5044 (1988).

[28] P. Miskiewicz, S. Kotarba, J. Jung, T. Marszalek, M. Mas-Torrent, E. Gomar-Nadal, D. B. Amabilino, C. Rovira, J. Veciana, W. Maniukiewicz, and J. Ulanski, J. Appl. Phys. **104**, 054509 (2008).

[29] Y. Lin, J. E. Eldridge, J. M. Williams, A. M. Kini, and H. H. Wang, Spectrochim. Acta, Part A **55**, 839 (1999).

[30] A. Lewandowicz, J. Rudzinski, L. Tronstad, M. Widersten, P. Ryberg, O. Matsson, and P. J. Paneth, Am. Chem. Soc. **123**, 4550 (2001).

[31] A. P. Scott and L. Radom, J. Phys. Chem. **100**, 16502 (1996).

[32] X. Linda Chen, A. J. Lovinger, Z. Bao, and J. Sapjeta, Chem. Mater. **13**, 1341 (2001).

[33] C. Reese and Z. Bao, Adv. Mater. (Weinheim, Ger.) **19**, 4535 (2007).

[34] R. W. I. de Boer, M. E. Gershenson, A. F. Morpurgo, and V. Podzorov, Phys. Status Solidi A **201**, 1302 (2004).